Applied Radiation and Isotopes, vol. 226, p. 112105, December 2025

Accepted manuscript: https://doi.org/10.1016/j.apradiso.2025.112105

Bioindication of radioactive contamination by honey bees in the Bryansk and Rostov regions: Foraging dynamics of ^{137}Cs and ^{40}K in the plant–bee–bee product pathway

Philip G. Sorokin

Although some studies have investigated the accumulation of radionuclides in honey, other bee products such as wax and bee bread remain insufficiently studied, particularly in terms of seasonal and intra-seasonal dynamics. Spatial patterns of contamination within the foraging area of honey bees, as well as the role of botanical composition of nectar sources, also remain poorly understood. This study examines the dynamics of ^{137}Cs and ^{40}K accumulation along the pathway plant–bee–bee product on radioactively contaminated territories in the Bryansk Region during different periods of the honey flow. The results are compared with data collected at low-contamination sites in the Rostov Region. Samples of honey, capping wax, and nectariferous plants were collected in the villages of Vereshchaki and Katichi (Bryansk Region), as well as in the stanitsa of Vyoshenskaya (Rostov Region). The equivalent gamma-dose rate was also measured in the vicinity of the Bryansk apiaries. The activity concentrations of ^{137}Cs and ^{40}K in plants and bee products were determined using gamma spectrometry. Statistically significant differences in the activity concentration of ^{137}Cs in honey samples from the Bryansk and Rostov regions were identified during different phases of the honey flow. In honey collected from contaminated areas (soil contamination density of ^{137}Cs ranging from 185 to 555 kBq/m^2), the mean activity concentration of ^{137}Cs was 44 ± 24 Bq/kg (range: 21–89 Bq/kg), significantly exceeding that of the control group. In capping wax, the mean activity concentration reached 56 ±

Philip G. Sorokin (philip.sorokin@gmail.com): Moscow State Academy of Veterinary Medicine and Biotechnology – MVA Named After K. I. Skryabin, Moscow, Russia.

33 Bq/kg (range: 29–115 Bq/kg). Pollen analysis and direct foraging tracking linked notably elevated ^{137}Cs activity concentrations in honey to nectar from *Brassica* spp. (rapeseed, field mustard), *Phacelia tanacetifolia*, *Melilotus* spp. (white/yellow sweet clover), *Trifolium* spp. (white/yellow clover), *Centaurea* spp. (cornflower, false-phrygian knapweed), *Symphytum officinale* (common comfrey), *Filipendula ulmaria* (meadowsweet), *Calluna vulgaris* (common heather), and *Solidago virgaurea* (European goldenrod), indicating the species-specific ability of these plants to accumulate radiocaesium and their potential as bioindicators of localized contamination hotspots. No statistically significant differences in the activity concentrations of ^{40}K in honey were observed between the regions. Higher variability and greater accumulation of radionuclides were found in capping wax compared to honey, likely due to biophysical filtration processes and differences in the physicochemical properties of honey and wax matrices. Transfer factors for ^{137}Cs and ^{40}K along the pathway nectariferous plant–honey/wax were calculated. For ^{137}Cs, arithmetic mean activity concentrations were used in the control group (homogeneous contamination), while weighted means were applied in the experimental groups (heterogeneous contamination) to account for spatial variability. A marked difference was found in ^{137}Cs concentrations in plants between the experimental groups (237 Bq/kg) and the control group (45 Bq/kg), while the transfer factors for ^{137}Cs remained consistent: 0.16–0.19 for honey and 0.24–0.44 for wax, suggesting the stability of these indicators under varying contamination conditions. The weighting of plant sample contributions was based on a digital area estimation of bee foraging zones, using pixel-wise analysis of masked regions on satellite imagery. Transfer factors for ^{40}K were calculated using pooled samples due to its uniform distribution across all settlements, yielding values of 0.05 for honey and 0.19 for wax. Partitioning analysis in a modern hive system was conducted, reflecting the mass-based distribution of radionuclides within the trophic system of honey bees. These results advance understanding of radionuclide distribution in agroecosystems and confirm the effectiveness of using honey bees and bee products as bioindicators of radioactive contamination across territories with both high and low contamination densities.

Keywords: *Bioindication of radioactive contamination; Honey bees; Radionuclide migration; Bee products; Honey; Capping wax; Radiation monitoring; Biomonitoring.*

1. INTRODUCTION

The honey bee (*Apis mellifera*) is known to be an effective bioindicator of radioactive and anthropogenic contamination in the environment (*Bargańska et al., 2015; Herrero-Latorre et al., 2017*). Investigating the migration of radionuclides along the plant–bee–bee product pathway is a critical component of radiation monitoring, enabling comprehensive assessments of ecological conditions in both individual ecosystems and the broader environment.

Following the Chernobyl nuclear power plant (ChNPP) accident in 1986, a substantial portion of radiocaesium fallout was deposited in the Bryansk Region, where localized areas of elevated soil contamination remain to this day. Radiocaesium (^{137}Cs), with a physical half-life of approximately 30.17 years, is the primary contaminant in the region. The regional mean density of ^{137}Cs contamination following the accident was 133 kBq/m^2, exceeding the pre-accident background level by a factor of 100. In the most heavily affected area—Novozybkov District—the mean contamination density reached 774 kBq/m^2 (*Vorobyev et al., 1994*).

The long-term presence of ^{137}Cs in ecosystems continues to pose a relevant challenge to radiological safety, despite the passage of decades and implementation of countermeasures. This issue remains relevant in all countries affected by radioactive fallout from the ChNPP disaster. The biomonitoring method using honey bees, which was tested in the present study in the well-characterized ^{137}Cs-contaminated zones of the Bryansk Region, can also be applied to other regions for the identification of contamination hotspots resulting from technological accidents, radioactive waste disposal, nuclear weapons testing, or nuclear energy production.

Potassium and cesium are alkali metals of Group IA, sharing similar physicochemical properties. As a result, they behave similarly in biological systems, making the study of potassium distribution as a biological analog of cesium scientifically relevant. A primary source of ^{40}K in the environment is the application of potassium fertilizers in agriculture.

Honey bees collect nectar and pollen, as well as honeydew and plant secretions, which are used to produce honey, wax, bee bread (fermented pollen known as *perga*), propolis, royal jelly and other hive products. Radionuclides enter these products via trophic transfer and accumulate within them, enabling the use of bees and their products in bioindication of radioactive contamination. The key advantages of this method include its high practical accessibility and broad spatial coverage. In their nectar-gathering process, honey bees cover an area of more than 20 km^2. Since various nectariferous plants bloom at different times and in different locations over the summer season, radionuclide monitoring at apiaries should be conducted continuously throughout the entire foraging season for maximal data acquisition and spatial resolution.

The objective of this study was to assess the foraging dynamics of ^{137}Cs and ^{40}K interrelated system along the plant–bee–bee product pathway in contaminated areas of the Bryansk Region and to compare the results with data from low-contamination zones in the Rostov Region. The study was conducted from May to September 2024 in the villages of Katichi and Vereshchaki (Novozybkov Urban District, Bryansk Region), and in the stanitsa of Vyoshenskaya (Sholokhov District, Rostov Region).

The study objects included bee products—honey and capping wax—collected from apiaries at different honey flow stages, as well as nectariferous plants sampled in the surrounding areas. The practical tasks comprised determining the activity concentrations of ^{137}Cs and ^{40}K in bee products and local nectariferous plants, along with measuring the equivalent dose rate of gamma radiation at the study sites.

2. MATERIALS AND METHODS

2.1. Study sites and sample collection

Samples of honey and capping wax were collected from private apiaries located in the village of Vereshchaki (Bryansk Region; Group 1, experimental), the village of Katichi (Bryansk Region; Group 2, experimental), and the stanitsa of Vyoshenskaya (Rostov Region; Group 3, control). The settlements associated with the experimental groups fall within the “zone of residence with the right to resettlement” (*Russian Federation, 1991; Russian Federation, 2023*), where current soil contamination density by ^{137}Cs ranges from 185 to 555 kBq/m^2. The apiaries in Vereshchaki and Katichi are situated 185 km and 182 km northeast, respectively, of the ChNPP fourth reactor unit. These two apiaries are separated by a distance of approximately 11 km (Fig. 1).

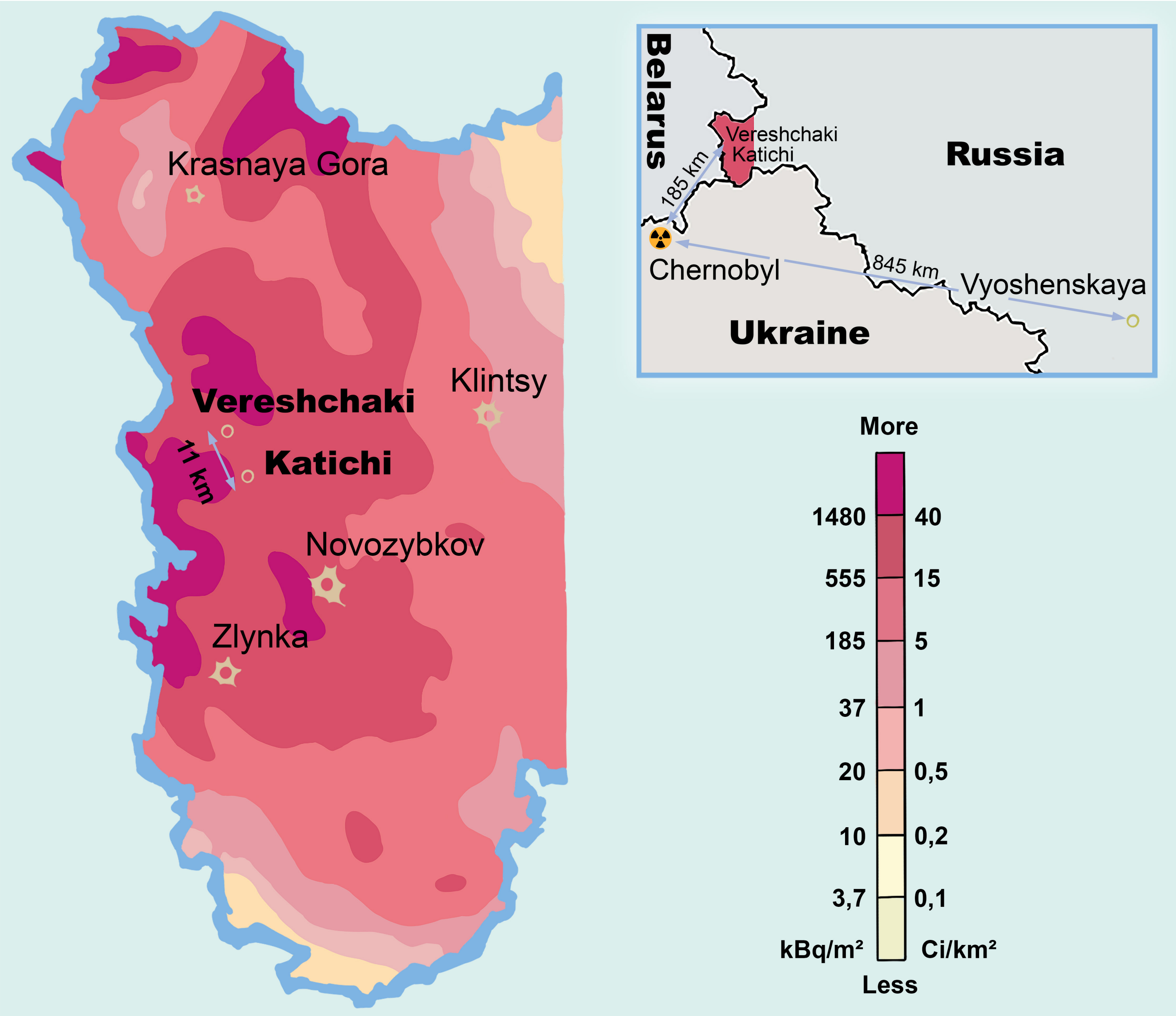

Fig. 1. Soil contamination with ^{137}Cs in the Bryansk Region in 1986.

Fig. 1 was developed using graphic design applications, based on published data (*Israel and Bogdevich, 2009*).

The control site, the stanitsa of Vyoshenskaya, is located 845 km southeast of the ChNPP's fourth reactor unit. Following the Chernobyl accident, ^{137}Cs contamination levels in the Rostov Region averaged 3.7–18.5 kBq/m^2 and did not exceed 33.3 kBq/m^2 (*Buraeva et al., 2022*).

During honey harvesting, honey from all hives was combined into a single container. Similarly, capping wax was collected progressively, stored in a common container, and melted down to produce wax. Thus, during each honey flow period, composite samples of honey and wax were formed, from which average subsamples were taken for analysis.

Group 1 consisted of *Apis mellifera carnica* and hybrid *A. m. mellifera* (15 hives), Group 2 included *A. m. caucasica* (15 hives), and Group 3 included *A. m. carnica*, *A. m. carpatica*, and *Buckfast* bees (130 hives). The experimental apiaries were stationary and remained fixed at their respective locations in the Bryansk Region, whereas the control apiary was migratory. During each honey flow period, it was relocated within a radius of no more than 400 km from Vyoshenskaya.

To ensure a more diverse floral base, the control apiary was subdivided into three groups, each transported to different locations at the same time. This migratory setup allowed broader coverage of the Rostov Region and provided a more comprehensive picture of the regional radiological environment. In contrast, the stationary apiaries located in radioactively contaminated areas of the Bryansk Region more accurately reflect local radiological conditions in geographically limited areas with high contamination density.

2.2. Climatic and meteorological characteristics of the study areas

The studied settlements in the Bryansk and Rostov regions are located in a temperate continental climate zone. Winters are cold and snowy, with air temperatures occasionally dropping to −20 °C or lower. Average January temperatures range from −7 °C to −9 °C. Summers are warm and moderately humid, with average July temperatures ranging from +20 °C to +24 °C and maximums exceeding +30 °C. Spring and autumn are well-defined, characterized by gradual changes in temperature. Spring typically begins in March, autumn in September. The growing season lasts approximately 5.7 months (173 days), generally from April 21 to October 11.

Annual precipitation ranges from 550 to 650 mm. Precipitation is relatively evenly distributed throughout the year, with a slight increase during the summer months (June and July), when heavy rains may occur. Snow cover usually forms in late November and persists until March, with the greatest depth observed in January and February. Wind speeds typically range between 10 and 18 km/h.

The further analyzed weather data were collected by member states of the World Meteorological Organization (WMO) and are shared under the terms of WMO Resolution 40 (*Meteostat, 2025*). Data for the stationary Groups 1 and 2 were obtained primarily from the weather station in Krasnaya Gora, located 30–38 km from Vereshchaki and Katichi, and partially from the weather station in Unecha, 64–69 km away. Average values for the migratory Group 3 were compiled from multiple weather stations located within a 400 km radius of the stanitsa of Vyoshenskaya, in accordance with the movement routes of the migratory apiary.

2.3. Gamma dose rate measurements and plant sampling

Measurements of equivalent dose rate (EDR) and sampling of mixed nectariferous plants were carried out in the immediate vicinity of the apiaries, in areas regularly visited by the bees from the study groups. EDR was measured using a scintillation dosimeter-radiometer (SRP-68-01). The aboveground parts of the plants were sampled in full using the envelope method at five locations within a 1-ha area in meadows and floodplains of the Iput River. Plants were first cleaned of soil residues, then dried in a laboratory oven at 105 °C until constant dry weight was achieved, and subsequently ground using an electric grinder.

Melted capping wax samples were also ground to a granular consistency, while honey was analyzed in its original form. Capping wax was sampled three times from each apiary—in June, August, and September. Honey was harvested six times at the apiaries of Groups 1 and 2. In Group 3, honey was harvested ten times due to the greater number of hives at the apiary. The flowering periods of the examined honey varieties overlapped, and most honey was polyfloral in origin, with dominant nectar sources varying by location. These are detailed in Table 1.

Table 1

Characteristics of the Investigated Honey Samples

No.	Vereshchaki, Bryansk Region (Group 1)		Katichi, Bryansk Region (Group 2)		Vyoshenskaya, Rostov Region (Group 3)	
	Sampling Date	Major Nectar Sources	Sampling Date	Major Nectar Sources	Sampling Date	Major Nectar Sources
1	17 May	Rapeseed, fruit trees, garden plants, willow	30 May	Rapeseed, fruit trees, garden plants, willow	15 May	Acacia, fruit trees, garden plants
2	15 June	Linden, sweetclover	12 June	Dandelion, buckthorn, raspberry, meadow grasses	30 May	Acacia, boxelder
3	05 July	Phacelia, rapeseed, field mustard, common comfrey, clover, sweet clover	20 June	Meadow grasses, raspberry	15 June	Sweet clover
4	15 July	Clover, meadow grasses	05 July	Rapeseed, field mustard, clover, sweet clover, phacelia, cornflower	25 June	Phacelia
5	15 Aug.	Clover, burdock, white sweet clover	05 Aug.	Phacelia, sow thistle, meadow and riparian herbs	08 July	Phacelia, sweet clover, motherwort
6	18 Sept.	Heather, goldenrod, field mustard, clover, sweet clover, meadowsweet	16 Sept.	Heather, goldenrod, phacelia, field mustard, knapweed, cornflower, clover, sweet clover	15 July	Motherwort, sage, valerian, coriander
7	–	–	–	–	15 July	Fireweed, sweet clover
8	–	–	–	–	25 July	Linden, raspberry
9	–	–	–	–	15 Aug.	Sunflower
10	–	–	–	–	15 Sept.	Goldenrod, garden plants

The botanical composition of honey was determined by monitoring the foraging activity of bees within the study area, tracking their primary foraging routes, followed by botanical identification of nectariferous plants. Additionally, melissopalynological (pollen) analysis of honey was conducted under laboratory conditions (*EASC, 2014; PalDat, 2024*). Pollen analysis excluded anemophilous plants (*Poaceae*) detected in autumn samples but not utilized as nectar sources — along with species flowering outside honey flow periods. While melissopalynology effectively identifies monofloral honeys, its accuracy for polyfloral varieties is inherently probabilistic. Hence, polyfloral honey assessment requires integrated analysis accounting for: pollen spectra (including potential sedimentation of heavier grains), direct foraging routes, filtration effects during honey processing, in-hive pollen storage patterns, and nectar plant phenology. Dominant autumn nectar sources (*Calluna vulgaris*, *Solidago virgaurea*) — though underrepresented in pollen spectra — were included as primary contributors, as pollen absence doesn't preclude nectar collection since bees can forage pollen and nectar from distinct sources.

2.4. Calculation of radionuclide transfer factors along the plant–product pathway

Transfer factors (TF) for radionuclides along the pathway nectariferous plant–honey/wax were calculated using a standard methodology according to the following equation:

$$TF = \frac{A_{product}}{A_{plants}}$$

where

$A_{product}$ — arithmetic mean activity concentration of the radionuclide in the product (Bq/kg), A_{plants} — arithmetic mean activity concentration of the radionuclide in plants (Bq/kg, dry weight basis), calculated for ^{40}K across all groups, and for ^{137}Cs in the control group.

In the experimental groups, instead of using the arithmetic mean, the weighted mean activity concentration of ^{137}Cs in plants was applied. It was calculated using a classical formula with weighting coefficients that account for the spatial heterogeneity of ^{137}Cs contamination across different land cover types within the foraging area of the bees:

$$A_{plants} = \frac{\sum(W_i \cdot A_i)}{\sum W_i}$$

where:

A_i — activity concentration of ^{137}Cs in the dry biomass of the sample (Bq/kg), W_i — weighting coefficient of the sample, calculated as:

$$W_i = \frac{S_i}{S_{total}} = \frac{S_i}{N(\pi R^2)}$$

where:

S_{total} — total area (km2) of the bee foraging territories,

N — number of apiaries in experimental groups (equal to the number of foraging zones),

R — effective foraging radius for stationary apiaries, assumed to be 3 km (*Palmer et al., 2024; Kendall et al., 2022*),

S_i — total area (km^2) of the land cover type from which the plant samples were taken. This value was determined using a digital approximation of double integration over the area, based on pixel summation from the map:

$$S_i = \iint_{\Omega} dA = k^2 N_{px}$$

where

k — image scale (km/px),

N_{px} — total number of pixels in the binary mask, determined as:

$$N_{px} = \sum_{x,y} M_{ROI}(x, y)$$

A satellite image of the study area was obtained using Google Earth™ and exported as a PNG file with a resolution of 2244 × 2244 px. A binary mask was manually applied to highlight the floodplain and adjacent lands excluded from agricultural use; the relevant region was filled with red (Fig. 2).

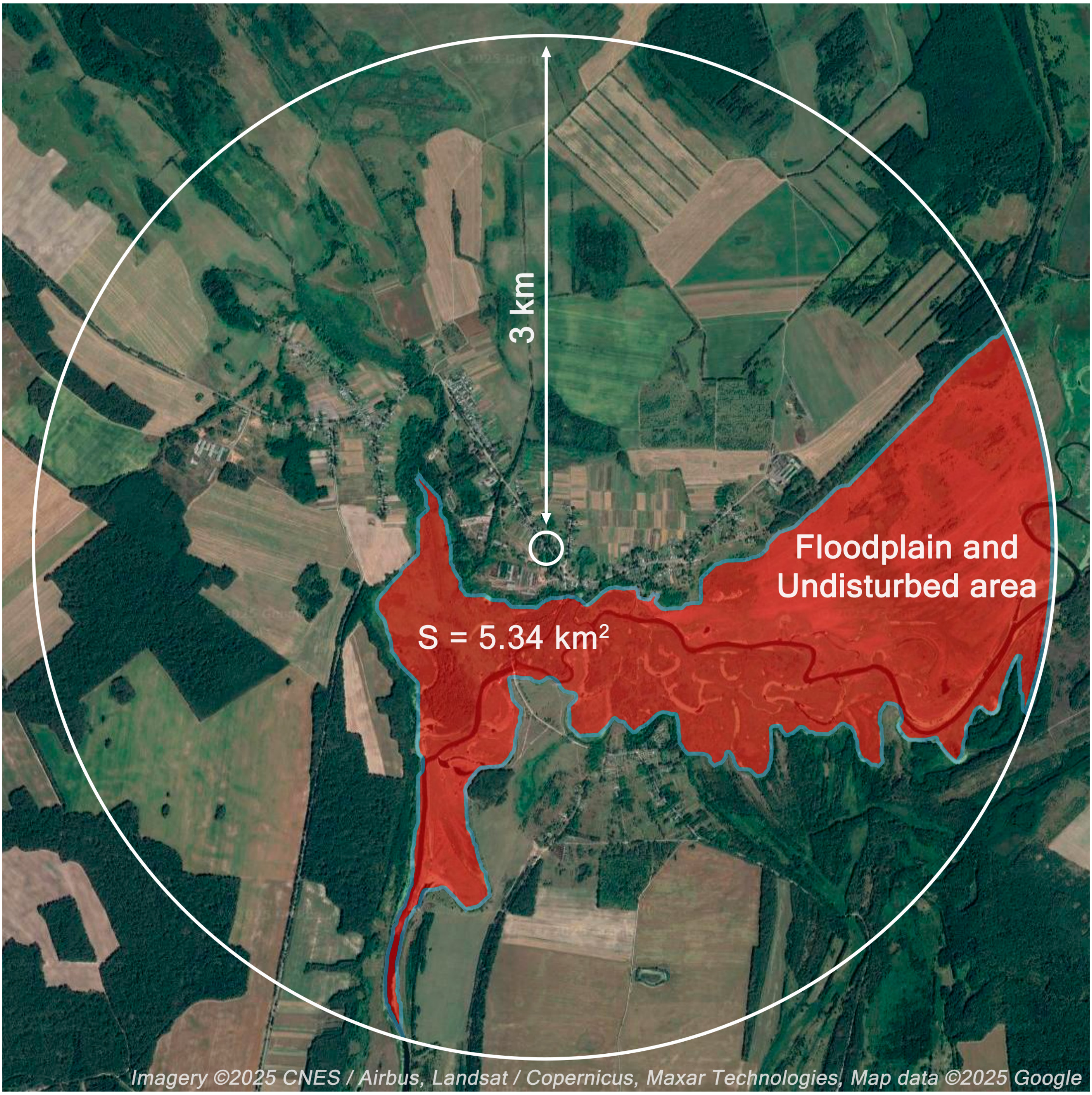

Fig. 2. Classification of foraging area by land types in Katichi vilage (Group 2).

At the center of the image, corresponding to the apiary coordinates, a white circle with a radius of 3 km was placed to define the area of interest. This circle was extracted using RGB color channel thresholds (R, G, B > 200) and approximated by the equation:

$$(x - a)^2 + (y - b)^2 = R_{px}^2$$

The least-squares method yielded a center at *(a, b) = (1119, 1121) px, with a radius of* R_{px} = *1055 ± 3 px.* Taking the actual radius as 3 km, the image scale was calculated as $k = 2.842 \cdot 10^{-3}$ *km/px = 2.84 m/px; so that Δx = 2.84 m*:

$$k = \frac{3\ km}{R_{px}}$$

The binary mask was defined as all pixels satisfying both the red-color threshold and spatial inclusion within the area of interest:

$$M_{ROI}(x, y) = [R > 150 \wedge G < 100 \wedge B < 100] \wedge \left[(x - a)^2 + (y - b)^2 < R_{px}^2\right]$$

For visual clarity, additional elements such as transparency overlays, mask contours, labels, lines, a central circle, and other annotations were added to the figure. These additions did not affect the original binary mask used for calculations. The image was finalized in graphic design applications. All numerical computations were performed in the *Python 3* environment using the libraries: *NumPy*, *Pillow*, and *scikit-image*.

2.5. Gamma spectrometry and statistical analysis

The activity concentrations of radionuclides in the analyzed samples were determined using gamma spectrometry using an SKS-99 "Sputnik" NaI(Tl) scintillation spectrometer with the "Progress" software suite (measurement range: 3–10^4 Bq for ^{137}Cs). The spectrometer was prepared according to the manufacturer's recommended protocol (*Amplituda Research & Technology Center LLC, 2014*): 15-min warm-up, calibration using a ^{22}Na reference source, and background measurement for 60 min. Each sample was measured over 30 min using a Marinelli beaker (volume: 500 cm^3). The average sample masses were approximately 700 g for honey, 470 g for capping wax and 120 g for dried plants.

Statistical analyses included descriptive and non-parametric methods implemented in computational statistics packages. Results are presented as mean ± SD. The Shapiro–Wilk test revealed deviations from normal distribution in the datasets; therefore, the Kruskal–Wallis test was used to assess differences between sample means. In cases where the null hypothesis was rejected, post hoc pairwise comparisons were conducted using Dunn's test with Bonferroni correction. The significance level was set at $p < 0.05$.

3. RESULTS AND DISCUSSION

3.1. Background gamma radiation levels and radionuclide content in plants

Table 2 presents the results of EDR measurements at open sites near the apiaries in Vereshchaki and Katichi (Groups 1 and 2), with published EDR values for natural areas in the Rostov Region. Gamma background levels in Groups 1 and 2 exceed the typical values for flat areas in the European part of the Russian Federation (0.08–0.15 μSv/h) and are characteristic for this region.

Table 2

EDR at open sites near apiaries

Locality (Region)	n	EDR, μSv/h
Vereshchaki (Bryansk Region)	10	0.37 ± 0.13
Katichi (Bryansk Region)	13	0.42 ± 0.15
Natural areas of Rostov Region*	1003	0.12 ± 0.04

*Source: *Buraeva et al., 2022*

Table 3 presents the results of gamma spectrometric analysis of ^{137}Cs and ^{40}K in nectariferous plants sampled in Vereshchaki, Katichi, and Vyoshenskaya, alongside reference values from published data for the Rostov Region.

Table 3

Activity concentrations of ^{137}Cs and ^{40}K in nectariferous plants (Bq/kg, dry mass)

Locality	Land Type	n	^{137}Cs	^{40}K
Vereshchaki (Bryansk Region)	Meadow (mixed forest zone)	5	178 ± 61	1636 ± 528
Katichi	Meadow (mixed forest zone)	5	163 ± 62	1651 ± 430
(Bryansk Region)	Floodplain (mixed forest zone)	5	1490 ± 650	1077 ± 416
Vyoshenskaya (Rostov Region)	Meadow (forest-steppe zone)	5	45 ± 20	1270 ± 483
Natural and Technogenic Territories, Rostov Region*	Dry steppe zone	55	14 ± 6	150 ± 62

*Source: *Buraeva and Bezuglova, 2023*

A comparative analysis of four sites — two meadow biotopes in the Bryansk Region (Vereshchaki and Katichi), a floodplain site near the Katichi River, and a control meadow in the stanitsa of Vyoshenskaya (Rostov Region) — revealed pronounced spatial heterogeneity in ^{137}Cs contamination. The highest levels of radiocaesium were recorded in the floodplain phytomass of Katichi. The meadows of the Bryansk Region showed significantly lower ^{137}Cs concentrations, although they remained statistically higher than the control values observed in Vyoshenskaya. No statistically significant difference in ^{137}Cs activity was found between the meadow sites in Vereshchaki and Katichi.

The activity concentration of ^{40}K was consistent across all study sites, indicating a stable potassium background and the absence of pronounced geochemical contrasts. Thus, ^{137}Cs demonstrated the highest spatial variability, while potassium (^{40}K) exhibited uniformity across the studied ecosystems.

A special case was represented by the dry steppe zone of the Rostov Region, where phytomass exhibited significantly lower concentrations of all radionuclides compared to both experimental and control sites located in the forest-steppe and mixed forest zones. The plant community of this zone was dominated by grasses such as feather grass (*Stipa capillata*, *Stipa ucrainica*, *Stipa lessingiana*), fescue (*Festuca valesiaca*), crested wheatgrass (*Agropyron cristatum*), and narrowleaf bluegrass (*Poa angustifolia*). *Psammophytic tumbleweed* species also played a significant role, including *Crambe* spp., *Gypsophila paniculata*, *Phlomis pungens*, and *Limonium* spp. The dominant species included *Artemisia lerchiana* and *Bassia prostrata*, along with the participation of *Camphorosma monspeliaca* and *Artemisia pauciflora*. Honey harvesting was not conducted at these sites due to the absence of a nectariferous base.

Following the deposition of radioactive fallout resulting from the Chernobyl accident, a range of rehabilitation measures were implemented in the Bryansk Region, including engineering decontamination, soil remediation, and reduction of radionuclide TFs to plants and animal products. These measures allowed for the return of a significant portion of radioactively contaminated land to agricultural use by 1992, with the transfer coefficients of anthropogenic radionuclides to forage crops for livestock reduced by a factor of 4–12. As a result, by 1993, the concentration of radionuclides in milk and meat produced in the region did not exceed permissible levels in 98.6 % and 100 % of cases, respectively (*IAEA, 2001*).

The most effective agrotechnical methods for the remediation of radioactively contaminated soils, applied in the Bryansk Region after the Chernobyl accident on agricultural lands and within populated areas, included the removal of the contaminated topsoil layer followed by its burial in disposal sites, and deep ploughing, in which the upper contaminated layer was inverted and buried deeper into the soil profile (*Balonov et al., 2014*). For sod-podzolic soils of the Bryansk Region, which are characterized by a thin fertile layer (15–20 cm), deep ploughing was carried out by turning the soil below the arable horizon to a depth of 25 cm, exceeding the standard depth by 4–5 cm. Other widely used agroameliorative measures in the region included the application of potassium fertilizers and soil liming, aimed at reducing the transfer of radionuclides into plants (*Fesenko et al., 2017*).

The period required for the purification of soils from anthropogenic radionuclides depends not only on their physical half-lives but also on factors such as horizontal and vertical migration, geographical location, and soil type. The removal of radionuclides through harvested crops and grazing animals also contributes to soil decontamination. The effective half-life, which reflects the physical half-life in combination with migration processes and radionuclide removal through biomass, is significantly shorter on agricultural lands due to the implementation of radiological countermeasures and ongoing land use. This explains the substantial differences in the radionuclide content of plants growing on agricultural land or in populated areas compared to those growing on undisturbed (fallow) plots.

The study site, located on the floodplain of the Iput River, represents an undisturbed area. In this zone, soil decontamination measures were not implemented comprehensively, no agricultural activity took place, and radionuclide removal via crops or green fodder was virtually absent. Radiocaesium is effectively fixed by soil minerals and exhibits low vertical mobility. Its horizontal migration is also slow, but it becomes a significant factor in riverine ecosystems, where radiocaesium accumulates predominantly in bottom sediments and silt. The longest effective half-life of radiocaesium is observed in forest ecosystems, where it closely approaches its physical half-life due to strong fixation by clay minerals and markedly slower vertical migration (*Holiaka et al., 2025*).

After the Chernobyl accident, the spatial distribution of radionuclides was heterogeneous and patchy, influenced by meteorological conditions in the atmospheric boundary layer, the uneven intensity and distribution of precipitation during the passage of the radioactive cloud, terrain features, and other contributing factors. Artificial and natural radionuclides are absorbed from the soil by nectariferous plants, with TFs to inflorescences and floral nectaries varying depending on plant species, soil composition, and climatic conditions.

3.2. Foraging radius and nectar collection sites

As previously noted, the productive foraging range of worker bees for nectar and pollen is approximately 3 km and depends on the bee species, terrain features, and meteorological conditions. In the absence of nearby floral sources and under conditions of high competition with other colonies, bees may travel significantly farther. In some cases, the foraging radius can reach 6 km or more; however, such distances are energetically costly and typically occur under unfavorable conditions, such as drought periods. The bees from the studied groups collected nectar during various phases of the foraging season from plants growing on agricultural lands, meadows, in populated areas, on undisturbed (fallow) land, and in forest edge zones.

3.3. Radionuclide content in honey and capping wax

Table 4 presents the results of measuring the activity concentrations of ^{137}Cs and ^{40}K in composite honey samples collected during different foraging periods. The foraging numbers correspond to those in Table 1.

Table 4

Activity concentration of ^{137}Cs and ^{40}K in honey samples, Bq/kg

Foraging No.	n	^{137}Cs			^{40}K		
		Group 1	Group 2	Group 3	Group 1	Group 2	Group 3
1.	3	27 ± 2	21 ± 2	10 ± 2	64 ± 5	65 ± 4	67 ± 6
2.	3	38 ± 3	34 ± 2	8 ± 1	71 ± 6	65 ± 6	65 ± 6
3.	3	89 ± 7	41 ± 4	5 ± 1	65 ± 5	68 ± 6	63 ± 5
4.	3	21 ± 2	44 ± 4	6 ± 1	62 ± 4	66 ± 5	68 ± 6
5.	3	29 ± 3	31 ± 3	8 ± 1	65 ± 5	69 ± 6	68 ± 7
6.	3	77 ± 6	75 ± 7	7 ± 1	69 ± 6	66 ± 4	64 ± 6
7.	3	—	—	6 ± 1	—	—	65 ± 6
8.	3	—	—	6 ± 1	—	—	66 ± 5
9.	3	—	—	6 ± 1	—	—	62 ± 6
10.	3	—	—	6 ± 1	—	—	70 ± 7
Average	—	47	41	7	66	67	66
Std. dev.	—	29	19	1	3	2	2
CV (%)	—	61	45	22	5	2	4

Statistical analysis revealed that the differences in ^{137}Cs activity concentrations among honey samples were statistically significant. Pairwise post hoc comparisons identified significant differences between Groups 1 and 3, and Groups 2 and 3, while no significant difference was observed between Groups 1 and 2. These findings indicate a substantial difference in ^{137}Cs content between honey from apiaries in the Bryansk and Rostov regions, and an insignificant difference within the Bryansk Region itself.

In beekeeping practices in Western Russia, the foraging season is typically divided into early spring, spring, early summer, summer, late summer, and autumn periods (*Griazkin et al., 2018*). Each of these periods is associated with the flowering of particular nectariferous plant groups and corresponding nectar productivity. The dynamics of ^{137}Cs activity concentrations in honey samples from Bryansk apiaries exhibited increased levels during early summer and summer, followed by a decrease in late summer, and a subsequent increase in autumn (Fig. 3). Substantial deviations from the mean are supported by coefficients of variation ≥ 45%. The low CV (22 %) in honey from the Rostov Region indicates relatively uniform ^{137}Cs activity concentrations.

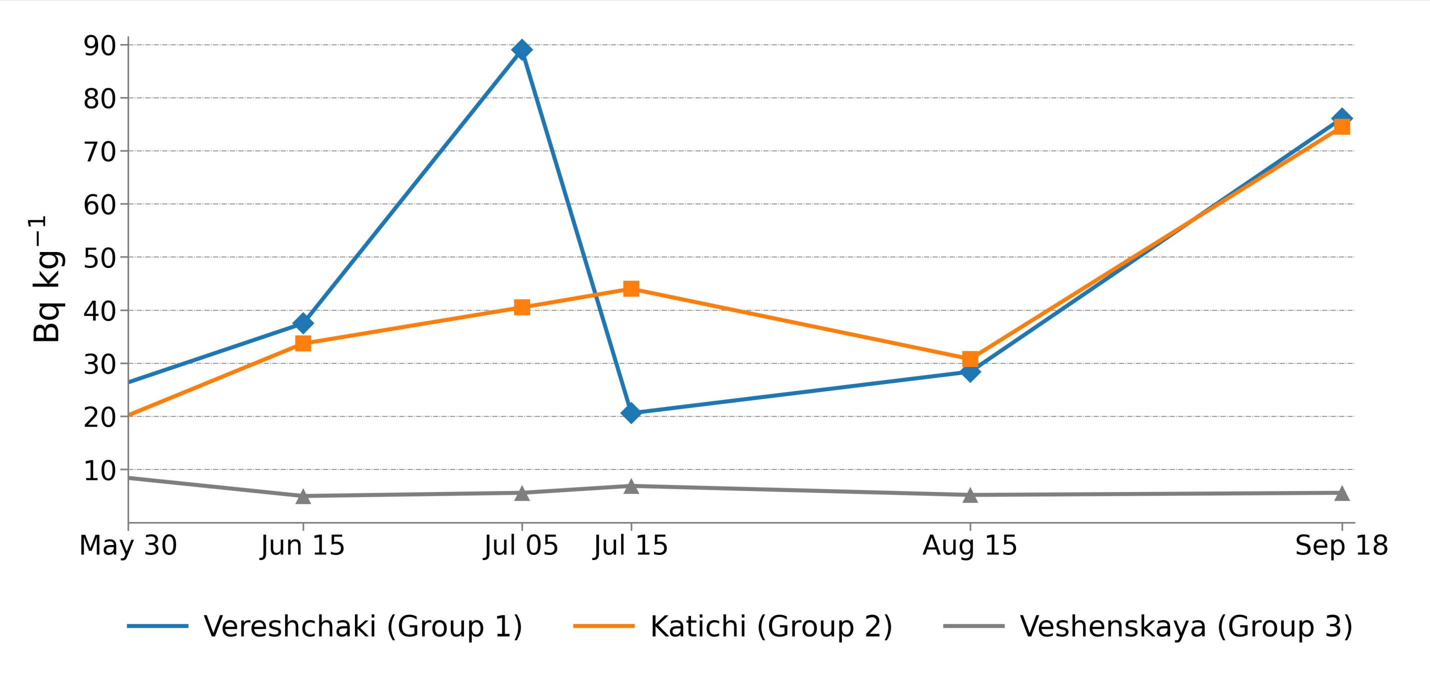

Fig. 3. Foraging dynamics of ^{137}Cs activity concentration in honey, Bq/kg.

Statistical analysis of ^{40}K activity concentrations in honey revealed no significant inter-group differences, indicating stable levels of this radionuclide across sampling periods. The low coefficients of variation (CV ≤ 5%) suggest limited fluctuation in ^{40}K activity concentrations (Fig. 4).

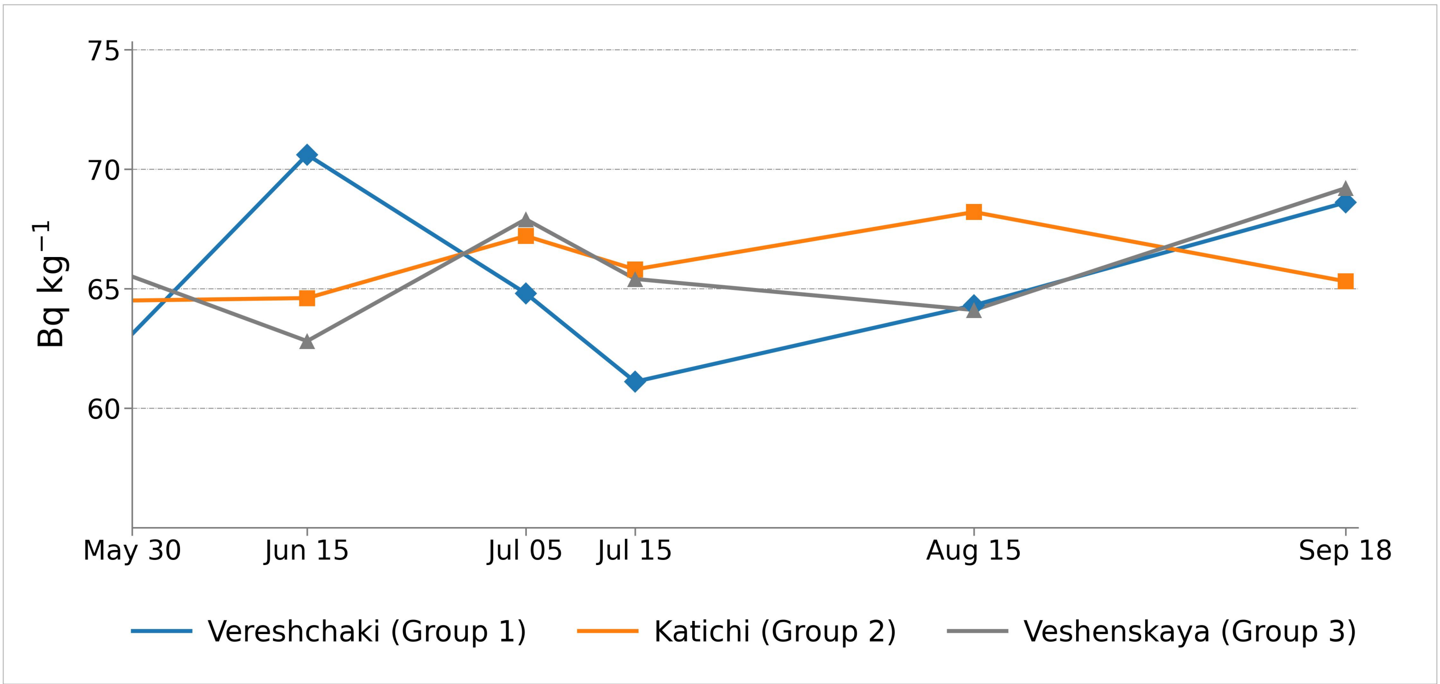

Fig. 4. Foraging dynamics of ^{40}K activity concentration in honey, Bq/kg.

Due to the fact that the rendering of capping wax was performed on-site once sufficient material had accumulated, only three temporal checkpoints of the foraging season were covered: May–June, June–August, and August–September. More frequent sampling and rendering of capping wax could have yielded additional data. Table 5 presents the activity concentrations of ^{137}Cs and ^{40}K in composite capping wax samples collected during different foraging periods.

Table 5

Activity concentration of ^{137}Cs and ^{40}K in capping wax samples, Bq/kg

Foraging No.	n	^{137}Cs			^{40}K		
		Group 1	Group 2	Group 3	Group 1	Group 2	Group 3
12–15 June	3	68 ± 5	33 ± 2	26 ± 3	243 ± 25	294 ± 27	260 ± 27
05–15 August	3	115 ± 9	29 ± 3	15 ± 2	244 ± 25	325 ± 30	404 ± 41
15–18 September	3	48 ± 5	41 ± 4	18 ± 2	189 ± 19	248 ± 25	247 ± 25
Average	—	77	34	20	225	289	304
Std. dev.	—	34	6	6	31	39	87
CV (%)	—	45	18	29	14	13	29

High coefficients of variation (CV > 33%) for ^{137}Cs in capping wax samples indicate substantial fluctuations in their activity concentrations over the foraging season. In contrast, ^{40}K showed consistent levels across all groups. Most sample sets demonstrated pronounced variability and higher accumulation of ^{137}Cs and ^{40}K in capping wax compared to honey. This can be attributed to the biological characteristics of bees, the sources of radionuclide intake, the physicochemical composition, and the mechanisms by which these products are produced by the bees.

3.4. Age-related specialization of honey bees and sources of radionuclide uptake in the trophic pathway

Honey bees are highly organized eusocial insects exhibiting a clear division of labor among individuals. In addition to caste differentiation (queen, drones, and workers), workers show age polyethism, whereby individuals sequentially assume different roles as they age. The lifespan of a worker bee depends on breed and environmental factors, ranging from 2 to 6 weeks in summer to an average of 20 weeks in winter (*Prado et al., 2020*). The phases of age-based specialization in *Apis mellifera* are summarized in Table 6 (*Johnson, 2010; Radchenko and Pesenko, 1994*).

Table 6

Age specialization of honey bees

Age (days)	Specialization	Functions
0–3	Cell cleaners	Clean cells of cocoons, feces, and other residues; may contribute to brood warming.
3–6	Young nurse bees	Digestive glands become active; feed older larvae (≥3 days) with bee bread and honey; wax glands begin developing.
7–11	Senior nurse bees	Development of hypopharyngeal (*G. hypopharyngeales*) and mandibular glands (*G. mandibulares*), responsible for producing royal jelly; feed young larvae and the queen; seal brood cells.
12–18	Middle-aged workers	Perform in-hive tasks: receive nectar and pollen from foragers, process nectar into honey, store food, build and seal combs, clean and ventilate the hive. Peak wax gland activity.
18–21	Guard bees	Transition phase to outdoor work; guard hive entrance, inspecting incoming insects. Foreign bees and pests are expelled.
>21	Foragers	Hypopharyngeal, mandibular, and wax glands degenerate. Sensory systems and flight muscles peak. Forage for nectar, pollen, water, and propolis.

Behavioral development in worker bees is pheromonally regulated and remains flexible, allowing for behavioral adjustments in response to colony needs. Colonies can regulate the nurse-to-forager ratio dynamically: in cases of forager loss, younger bees may begin foraging earlier; conversely, in the absence of brood care, older bees may revert to nursing duties, including partial regeneration of hypopharyngeal glands—a phenomenon described as behavioral reversion.

Unlike wild bees, honey bees maintained in managed apiaries live under more favorable conditions. Beekeepers provide hive maintenance, protection from predators, and preconstructed artificial combs known as foundation. These wax sheets are manufactured using molds with hexagonal impressions on both sides and are composed of standardized wax blends, including beeswax and commercial wax. As a result, bees expend less energy on comb construction, accumulate biomass more rapidly—which correlates directly with foraging efficiency—and may begin foraging 1–3 days earlier (*Huang and Robinson, 1996*). For guard bees, early foraging may also occur under low threat levels.

Nectar, pollen, and water are collected by foragers, whereas wax secretion is carried out primarily by middle-aged bees and, to a lesser extent, nurse bees. Nectariferous plants are the source of honey and pollen, whereas wax is a secretion of the bee's wax glands. Consequently, radionuclide accumulation in these products occurs via different pathways: while radionuclides enter nectar and pollen through plant uptake from contaminated soil, their entry into wax is linked to bioaccumulation and internal distribution within the bee organism.

Bees derive carbohydrates from honey and proteins from bee bread. Radionuclides accumulate in the body and are excreted through various pathways, including via wax glands. It is estimated that the production of 1 kg of wax requires the consumption of up to 8 kg of honey, implying that a substantial amount of radionuclides passes through the bee's body over time—a biological filtration effect. This may explain the observed differences in radionuclide content between honey and wax.

It is important to note that in managed apiaries, the biologically active wax product is capping wax, which bees use to seal honey and brood cells—not the industrial foundation wax, although foundation combs are partially extended by builder bees.

Honey bees interact with various environmental media—air, plants, and water—accumulating radionuclides via multiple pathways. Water is collected for hydration and hive thermoregulation. Bees also gather propolis for sealing hive crevices, reinforcing combs, and disinfection. Propolis is a lipophilic resinous matrix capable of accumulating radionuclides both directly from resin-producing plants and through the deposition of radioactive aerosols on hive surfaces following primary or secondary releases (e.g., during forest fires). Bees actively capture aerosol particles deposited on plant surfaces through electrostatic binding (*Meacci et al., 2025*). It is propolis and pollen that demonstrate high representativeness as bioindicators: after the Chernobyl accident, the concentrations of radionuclides in these bee products reached anomalously high levels (*Bogdanov, 2005*), consistent with their role as accumulators of anthropogenic radionuclides.

Thus, the informative value of bee-derived products in biomonitoring varies depending on the radionuclide source, type of contamination, and monitoring objectives. The transfer coefficients for radiocaesium into pollen are several times higher than into honey, not only immediately after fallout but also during long-term post-accident periods (*Barišić et al., 1992*). Conversely, radiocaesium content in propolis may decrease to levels similar to those in honey, though it depends on the collection site (forest vs. meadow). In delayed contamination scenarios, propolis can serve as an effective indicator of secondary releases.

Whereas honey, pollen, and propolis reflect radionuclide content via distinct environmental uptake routes, wax functions as an integrative indicator, accumulating radionuclides through biological filtration. Similarly, honey bees themselves serve as biological indicators, both in the immediate aftermath of primary or secondary releases and during later stages. Intra-colony variation in radionuclide accumulation across age cohorts of bees (e.g., ^{3}H, ^{57}Co, ^{60}Co, ^{54}Mn, ^{22}Na, ^{7}Be, ^{131}W) is negligible (*Haarmann, 1997*); however, foragers may represent a more sensitive indicator due to their exposure and aerosol-binding capacity via electrostatic attraction.

3.5. Characteristics of radionuclide accumulation in honey and capping wax

The increased activity concentrations and higher variability of ^{137}Cs and ^{40}K in capping wax compared to honey can be explained not only by biological filtration effects, but also by fundamental differences in phase states and the chemical composition of the matrices. Honey is a hydrophilic aqueous solution of carbohydrates, in which $^{137}Cs^{+}$ and $^{40}K^{+}$ cations remain mobile and are in dynamic equilibrium. In contrast, capping wax is composed primarily of wax esters (67%), aliphatic hydrocarbons (14%), free fatty acids (12%), and alcohols (1%) (*Svečnjak et al., 2019*), with trace amounts of propolis, honey, and pollen residues. This combination forms a dense hydrophobic matrix with pronounced ion-sorption properties.

During the secretion of liquid wax, radiocaesium and other cations present in the bee hemolymph are selectively sorbed by carboxyl and ester groups. Subsequent crystallization and the absence of free water effectively prevent the back-diffusion of ions, ensuring long-term retention of radionuclides within the wax structure.

Capping is formed through a series of short-term cell-sealing events, each lasting from several hours to a full day. Each act reflects the current radioecological load brought in with nectar, pollen, water, and aerosols collected during foraging. The heterogeneity of the botanical base and the variability of ion sorption at the time of wax secretion lead to pronounced fluctuations in radionuclide activity within individual wax scales. In the composite capping wax sample, these scales combine into a cumulative matrix with high dispersion of values. This explains the greater variability in the activity concentrations of ^{137}Cs and ^{40}K in wax compared to honey, where multi-day accumulation, solubility, and mixing in the cells smooth out radionuclide fluctuations.

While beyond the scope of this study, the bioindication of technogenically enhanced natural radionuclides (TENORM) remains scientifically relevant due to their accumulation in anthropogenically disturbed ecosystems and associated ecological risks. For instance, ^{226}Ra can enter the biosphere through offshore oil extraction, coal mining, fossil fuel processing and combustion, and sand refining (*Vearrier et al., 2009*). As a decay product of ^{238}U, ^{226}Ra is often found in elevated concentrations in mining residues. Fly ash from coal-fired power plants can contain high levels of ^{226}Ra and other TENORM, which may be transported via airborne particulates over distances up to 10 km (*Lovrenčić Mikelić et al., 2024*). Elevated concentrations of ^{232}Th are present in niobium and phosphate ores. Additional sources of ^{226}Ra and ^{232}Th include phosphate fertilizers, due to the association of these radionuclides with phosphorite ores, as well as construction waste, which may release radionuclides into the environment during processing. TENORM may also serve as indirect indicators of chemical pollution, as their release into the environment is often accompanied by broader technogenic contamination involving various pollutants.

The mechanism of radionuclide accumulation in honey and wax depends on their chemical characteristics. For ^{137}Cs and ^{40}K, which exist in ionic form and exhibit biological similarity, transfer to honey occurs primarily through the root pathway, while in wax, they accumulate during active wax secretion by the bees' wax glands. In the case of ^{226}Ra (a chemical analog of Ca^{2+}) and especially ^{232}Th (which forms insoluble compounds), adsorption of solid-phase particles plays a dominant role. These include pollen, mineral dust, and aerosols carried on the bees' bodies during contact with contaminated surfaces — a process linked to the aforementioned electrostatic binding of aerosols. In addition, pollen grains may accumulate radionuclides directly from the atmosphere.

Thus, the lipophilic matrix of wax determines its ability to accumulate not only radionuclides but also a wide range of trace elements, heavy metals, and pesticides (*Bommuraj et al., 2019*), confirming the role of wax as a key depot of environmental contaminants in the hive and underscoring its value as a sensitive and informative matrix for biomonitoring.

3.6. Potassium as a biological analog of radiocaesium in the soil–plant–bee product system

A recent study on the long-term ecological consequences of radiocaesium contamination from nuclear weapons testing (*Kaste et al., 2021*) demonstrated a negative correlation between potassium content in soil and ^{137}Cs activity in honey. Although the total potassium content in soil does not fully reflect its bioavailability to plants, it served as a regional-scale predictor of ^{137}Cs uptake. The study showed that in soils with low potassium content, the biological availability of ^{137}Cs increases, leading to its accumulation in plants and subsequent transfer into honey. In such regions, ^{137}Cs contributed significantly to the overall radioactivity of honey, in some cases exceeding the natural background created by ^{40}K. The very detection of "bomb" cesium 50 years later highlights the long-lasting nature of radioactive legacy and the sensitivity of biomonitoring methods. A statistically significant positive correlation between the activity concentrations of ^{40}K and ^{137}Cs was also reported in a subsample of 84 honey samples from the Fukushima area (*Inose et al., 2023*).

The natural isotopic composition of potassium remains virtually constant, with ^{40}K comprising approximately 0.0117 % of the total potassium. Variability in potassium isotope ratios in most terrestrial samples is extremely low and can only be reliably measured using high-precision methods with an accuracy better than 0.1 ‰ (*Wang et al., 2021*). These findings suggest that the isotopic composition of potassium in the studied biological system is likewise stable. Therefore, the activity concentration of ^{40}K in soil and honey correlates with the concentration of bioavailable potassium, which can be used to assess the potential influence of potassium on the transfer of radiocaesium along the soil–plant–hive product pathway.

In the present study, no statistically significant differences in the activity concentration of ^{40}K were observed between honey samples from experimental and control groups. The variability of ^{40}K content in capping wax was also minimal. Among plant samples collected from meadow and floodplain sites, no significant intergroup differences in ^{40}K activity concentration were found. Consequently, there is no evidence that potassium as a competing factor influenced ^{137}Cs accumulation in bee products in this study. The uniformity of ^{40}K levels in both honey and plant matrices, combined with consistently similar ^{137}Cs TFs, indicates that the dominant factors are the spatial heterogeneity of soil radiocaesium contamination along with the plant species composition, rather than potassium deficiency. Nevertheless, the use of ^{40}K as an endogenous indicator of potassium availability remains relevant for the comparative analysis of territories with contrasting potassium content.

3.7. Transfer and partitioning

Table 7 presents the results of transfer factor calculations for ^{40}K along the pathway plant–product, based on the combined dataset from the experimental and control groups, which were homogeneous in terms of radionuclide activity concentrations in plant, honey, and wax samples.

Table 7

Transfer factors for ^{40}K along the plant–product pathway

Radionuclide	Mean activity concentration in dry plants, Bq/kg (n = 20)	Mean activity concentration in product, Bq/kg		TF (plant → product)	
		Honey (n = 22)	Wax (n = 9)	Honey	Wax
^{40}K	1409 ± 496	66 ± 3	273 ± 62	0.05	0.19

Table 8 shows the transfer factors of ^{137}Cs along the plant–product pathway, calculated using the weighted mean activity concentration of ^{137}Cs in plants from the combined sample of experimental groups in the Bryansk Region. These groups showed no statistically significant differences in ^{137}Cs levels in honey.

Table 8

Transfer factors of ^{137}Cs along the plant–product pathway (experimental groups)

Radionuclide	Weighted mean activity concentration in dry plants, Bq/kg (n = 15)	Mean activity concentration in product, Bq/kg		TF (plant → product)	
		Honey (n = 12)	Wax (n = 6)	Honey	Wax
^{137}Cs	237	44 ± 24	56 ± 33	^{137}Cs	237

For the control group in the Rostov Region, transfer factors were calculated using the arithmetic mean activity concentration of ^{137}Cs in nectariferous plants (Table 9).

Table 9

Transfer factors of ^{137}Cs along the plant–product pathway (control group)

Radionuclide	Mean activity concentration in dry plants, Bq/kg (n = 5)	Mean activity concentration in product, Bq/kg		TF (plant → product)	
		Honey (n = 10)	Wax (n = 3)	Honey	Wax
^{137}Cs	45 ± 20	7 ± 1	20 ± 6	0.16	0.44

The obtained transfer factors for ^{137}Cs from plants to honey and wax in both experimental and control groups (0.16–0.19 for honey and 0.24–0.44 for wax) correspond well to the published range (0.18–0.36) for dry flower biomass (*Barišić et al., 1992*). This confirms the reliability of the calculations and demonstrates the high sensitivity of the bioindicator method even under low levels of radioactive contamination. The consistency of transfer factors across groups was also notable: the relative difference in TFs for honey was approximately 16%, and for wax about 45%. The larger variation in wax TFs is likely explained by the limited number of wax samples, though the difference remains acceptable.

The distribution of the total radionuclide mass between honey and wax is important for predictive modeling and radiological risk assessment. Table 10 presents partitioning factors between honey and capping wax, reflecting the distribution of the total radionuclide mass in bee-produced matrices. For ^{137}Cs, partitioning factors were calculated separately for the experimental and control groups and then averaged.

Table 10

Partitioning factors of ^{137}Cs and ^{40}K between honey and capping wax (modern hive system)

Radionuclide	Partitioning factor (%)	
	Honey	Wax
^{137}Cs	0.96	0.04
^{40}K	0.92	0.08

The gross wax yield under traditional beekeeping practices with active comb building may reach 15% or more of the total honey yield (*Aregawi et al., 2014*). However, in modern hives equipped with preformed foundation sheets, this yield is considered constant at approximately 2%. Thus, for every 1000 g of honey produced, bees secrete approximately 20 g of wax. Despite the higher activity concentration per kilogram in wax compared to honey, the total activity of radionuclides in wax amounts to 4.2% (cesium) and 8.7% (potassium) of that in honey.

When interpreting transfer and partitioning patterns, it is important to consider both the competitive effect of potassium on ^{137}Cs transfer in the soil–plant link and the non-root (aerial) pathway of radionuclide intake (including ^{137}Cs and others) into wax due to secondary emissions.

3.8. Influence of meteorological conditions and natural events

During the honey flow season, no forest fires, peat bog ignitions, or other natural emergencies were reported that could have introduced secondary radioactive contamination and confounded the study results. Table 11 presents meteorological data from the surveyed localities for the period from May 15, 2024 to September 18, 2024.

Table 11

Average daily meteorological data during the study period

Region	n	Air Temperature, °C			Precipitation, mm	Atmospheric Pressure, hPa	Wind Speed, km/h
		Average	Min	Max			
Bryansk Region (Groups 1 & 2)	127	20 ± 3	14 ± 3	26 ± 3	1.9 ± 4.8	1015 ± 6	12 ± 4
Rostov Region (Group 3)	127	23 ± 4	17 ± 4	29 ± 4	1.0 ± 1.9	1014 ± 6	13 ± 4

In 2024, honey harvesting in both Bryansk and Rostov regions took place under favorable warm weather conditions, with minor fluctuations in air temperature, wind speed, and atmospheric pressure, and negligible differences between experimental and control groups. These factors are therefore unlikely to have influenced the study results. Despite considerable variability in precipitation, total rainfall during the honey flow period in the surveyed settlements was below the regional climatic norm: 241 mm in Bryansk Region (norm: 280 mm) and 130 mm in Rostov Region (norm: 219 mm). Precipitation patterns in Bryansk Region during the study period are shown in Fig. 5.

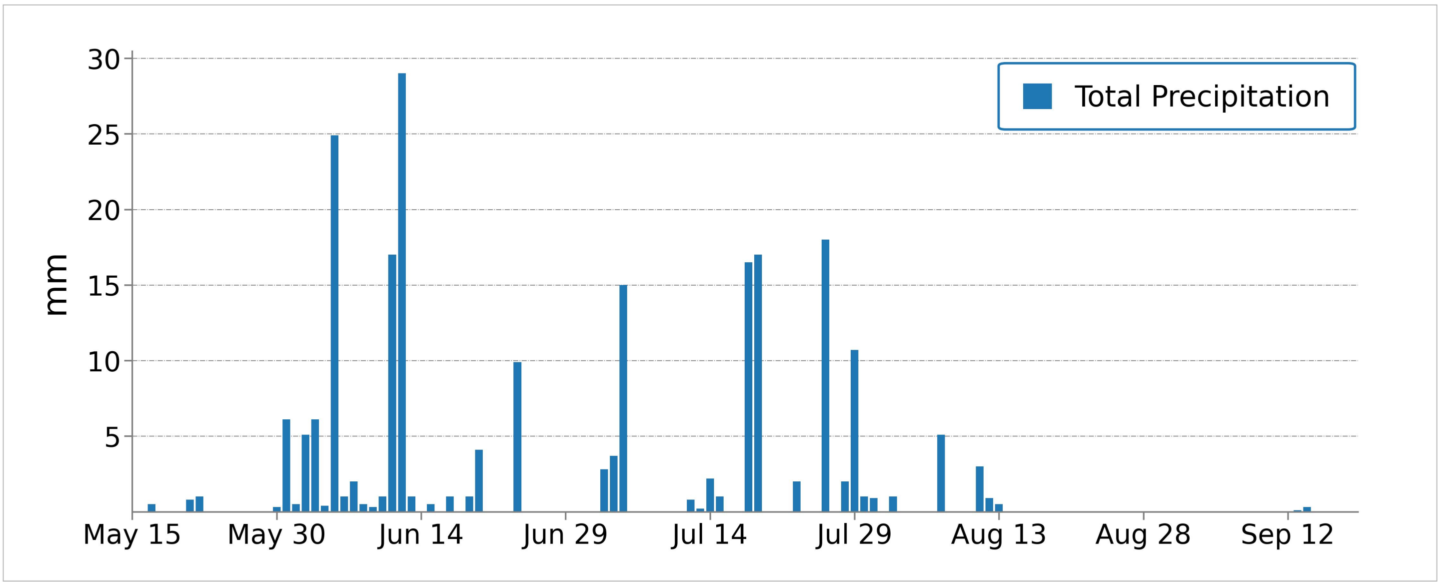

Fig. 5. Precipitation distribution in Bryansk Region during the study period, mm.

A comparison of precipitation dynamics with the foraging-related variation in radionuclide activity concentrations in honey did not reveal a clear dependency. From May to July, when precipitation levels were highest, ^{137}Cs activity in honey increased. However, a similar increase was observed from August to September, despite minimal rainfall. For ^{40}K, no discernible fluctuation in honey activity concentrations was observed. Given the similar physicochemical properties and biological kinetics of ^{40}K and ^{137}Cs, the stability of ^{40}K provides indirect evidence that meteorological factors did not measurably influence the transfer of ^{137}Cs from plants to honey. All study sites are located within the same climatic zone, making these findings applicable to the control group in the Rostov Region as well. Nonetheless, the response of ^{137}Cs concentration in inflorescences and floral nectaries to precipitation may differ depending on plant species and precipitation levels.

3.9. Influence of bee breed differences

No statistically significant differences in ^{137}Cs activity concentrations in honey were found between Groups 1 and 2, which comprised *A. m. carnica*, *A. m. mellifera*, and *A. m. caucasica* breeds. This suggests a lack of variation in ^{137}Cs accumulation across these genetic lines. Group 3 was more numerous and included a broader range of breeds that were not differentiated during sample collection. Therefore, in the absence of fluctuations in composite sample results, there is no basis to assume that similar breed-level uniformity applies to *A. m. carpatica* and *Buckfast* bees. Nonetheless, the overall trend supports the conclusion that bee breed did not significantly influence radionuclide accumulation in this study.

CONCLUSION

The foraging-related dynamics of ^{137}Cs migration along the plant–bee–bee product pathway in the radioactively contaminated territories of the Bryansk Region were characterized by increasing ^{137}Cs activity concentrations in honey collected during the early summer, summer, and autumn foraging periods. This trend likely reflects spatial heterogeneity in radionuclide contamination of nectar-producing habitats, differences in migration processes, and the varying capacity of plant species to accumulate radiocaesium.

Pollen analysis and direct foraging tracking linked notably elevated ^{137}Cs activity concentrations in honey to nectar from *Brassica* spp. (rapeseed, field mustard), *Phacelia tanacetifolia*, *Melilotus* spp. (white/yellow sweet clover), *Trifolium* spp. (white/yellow clover), *Centaurea* spp. (cornflower, false-phrygian knapweed), *Symphytum officinale* (common comfrey), *Filipendula ulmaria* (meadowsweet), *Calluna vulgaris* (common heather), and *Solidago virgaurea* (European goldenrod), indicating the species-specific ability of these plants to accumulate radiocaesium and their potential as bioindicators of localized contamination hotspots. In the control group, intra-seasonal variation in ^{137}Cs activity was low.

Statistically significant differences in ^{137}Cs activity concentration were observed between honey samples from the Bryansk and Rostov Regions, while no such differences were found between apiaries within the Bryansk Region. On experimental apiaries located in settlements with current soil contamination levels of 185–555 kBq/m^2 ^{137}Cs, the mean activity concentration in honey was 44 ± 24 Bq/kg (range: 21–89 Bq/kg), significantly exceeding values in the control group. In capping wax, the corresponding mean activity was 56 ± 33 Bq/kg (range: 29–115 Bq/kg).

The activity concentrations of ^{40}K in honey from the Bryansk and Rostov Regions did not differ significantly and remained stable throughout the observation period. This uniformity may reflect the absence of industrial sources of technogenic releases and the influence of ^{40}K-background radiation across the studied sites.

Significant differences in ^{137}Cs activity concentration in plant samples were found both between the experimental and control groups and among geologically distinct sampling sites within these groups. In contrast, the activity of ^{40}K was statistically uniform across all sites, with the exception of the dry steppe zone in the Rostov Region (where honey harvesting was not conducted). The weighted mean activity concentration of ^{137}Cs in nectariferous plants from the combined experimental groups was 237 Bq/kg, compared to the arithmetic mean 45 ± 20 Bq/kg in the control group.

Transfer factors for ^{137}Cs and ^{40}K along the plant–honey and plant–wax pathways were quantified, with ^{137}Cs TFs ranging from 0.16–0.19 (honey) and 0.24–0.44 (wax), consistent with published values, and ^{40}K TFs of 0.05 (honey) and 0.19 (wax). The narrow ^{137}Cs TF ranges demonstrate remarkable consistency across contrasting contamination landscapes: maintaining stability in both high-activity density sites and low-activity density areas, indicating environmental resilience of these transfer indicators. Partitioning analysis in a modern hive system was conducted, reflecting the mass-based distribution of radionuclides within the trophic system of honey bees.

^{137}Cs and ^{40}K exhibited greater variability and accumulation in capping wax than in honey, a pattern attributed to biological filtration and fundamental differences in the physicochemical composition of the wax and honey matrices. Due to the specifics of its secretion and deposition, capping wax reflects the current radioecological load from both root and non-root uptake pathways and serves as a highly sensitive medium for radiological monitoring. The results obtained contribute to a better understanding of ^{137}Cs and ^{40}K distribution in honey bee–

associated ecosystems, highlight the potential of identifying plant species that serve as effective markers of localized radioactive hotspots, and demonstrate the potential for using honey bees and their products as bioindicators of radioactive contamination in environments with both elevated and low levels of radionuclide deposition.

DECLARATION OF COMPETING INTEREST AND FUNDING

The author declare that they have no known competing financial interests or personal relationships that could have appeared to influence the work reported in this paper. This research did not receive any specific grant from funding agencies in the public, commercial, or not-for-profit sectors; all costs were covered by the author personally.

DATA AVAILABILITY

The source code and operational satellite map for determining ^{137}Cs activity weighting factors in plants, as well as pollen analysis protocols are available in the Mendeley Data repository (*Sorokin, 2025*). Other data will be made available on request.

REFERENCES

Amplituda Research & Technology Center LLC, 2014. Spectrometric Installation SKS-99 “Sputnik”: Operating Manual: Document code “МГФК.412154.001РЭ”. Moscow, pp. 4–10. https://www.doza.ru/docs/radiation_control/SKS-99_Sputnik.pdf (accessed 2025 May 17). (In Russian).

Aregawi, G., Tilahun, M., Gangwar, S.K., Gebresamue, G., Tesfay, G., 2014. Performance of Apis mellifera spp. on honey and beeswax production in different type of beehives in Enda Mekoni Woreda, Tigray Region, Ethiopia. *Global Journal of Bio-science and BioTechnology*. 3(3), 324–329.

Balonov, M.I., Golikov, V.Yu., Parkhomenko, V.I., Ponomarev, A.V., 2014. Decontamination of localities in the Bryansk region after the Chernobyl accident. *Radiation Hygiene.* 7(1), 5–15. (In Russian).

Bargańska, Ż., Ślebioda, M., & Namieśnik, J., 2015. Honey bees and their products: Bioindicators of environmental contamination. *Critical Reviews in Environmental Science and Technology.* 46(3), 235–248. https://doi.org/10.1080/10643389.2015.1078220.

Barišić, D., Lulić, S., Kezić, N., Vertačnik, A., 1992. ^{137}Cs in flowers, pollen and honey from the Republic of Croatia four years after the Chernobyl accident. *Apidologie.* 23(1), 71–78. https://doi.org/10.1051/apido:19920108.

Bogdanov, S., 2005. Contaminants of bee products. *Apidologie.* 37(1), 1–18. https://doi.org/10.1051/apido:2005043.

Bommuraj, V., Chen, Y., Klein, H., Sperling, R., Barel, S., Shimshoni, J.A., 2019. Pesticide and trace element residues in honey and beeswax combs from Israel in association with human risk assessment and honey adulteration. *Food Chemistry.* 299, 125123. https://doi.org/10.1016/j.foodchem.2019.125123.

Buraeva, E.A., Malomyzheva, N.V., Shvetsova, D.A., Bezuglova, O.S., 2022. Radionuclides in the Upper Soil Layer of Specially Protected Natural Territories of the Rostov Region. *Bulletin of Higher Educational Institutions. North Caucasus Region.* 3, 38–44. (In Russian).

Buraeva, E.A., Bezuglova, O.S., 2023. The Specific Activity of the Naturally Occurring Radionuclides and Artificially Produced ^{137}Cs in Soils and Herbaceous Plants of Rostov Oblast. *Arid Ecosystems.* 13, 65–72. https://doi.org/10.1134/S2079096123010031.

EASC (Euro-Asian Council for Standardization, Metrology and Certification), 2014. GOST 31769-2012 (Interstate Standard): Mjod. Metod opredelenija chastoty vstrechaemosti pyl'cevyh zjoren [Honey. Method for the determination of the frequency of occurrence of pollen grains]. Moscow, pp. 2–5. (In Russian).

Fesenko, S., Howard, B.J., Sanzharova, N., Vidal, M, 2017. Remediation of Areas Contaminated by Caesium: Basic Mechanisms Behind Remedial Options and Experience in Application. In: Gupta, D., Walther, C. (eds) Impact of Cesium on Plants and the Environment. Springer, Cham, pp. 265–310. https://doi.org/10.1007/978-3-319-41525-3_15.

Griazkin, A.V., Samsonova, I.D., Belyaeva, N.V., Belyaev, V.V., Gutal, Marko, Feklistov P.A., 2018. Potential of forest melliferous resources of northwest Russia. *Horticulture International Journal.* 2(6), 390–394. https://doi.org/10.15406/hij.2018.02.00082.

Haarmann, T.K., 1997. Honey bees as indicators of radionuclide contamination: exploring colony variability and temporal contaminant accumulation. *Journal of Apicultural Research.* 36(2), 77–87. https://doi.org/10.1080/00218839.1997.11100933.

Herrero-Latorre, C., Barciela-García, J., García-Martín, S., Peña-Crecente, R.M., 2017. The use of honeybees and honey as environmental bioindicators for metals and radionuclides: a review. *Environmental Reviews.* 25(4), 463–480. https://doi.org/10.1139/er-2017-0029.

Holiaka, D., Levchuk, S., Kashparov, V., Yoschenko, V., Hurtevent, P., Coppin, F., Beasley, J.C., 2025. ^{90}Sr and ^{137}Cs distribution in Chornobyl forests: 30 years after the nuclear accident. *Journal of Environmental Radioactivity.* 282, 107616. https://doi.org/10.1016/j.jenvrad.2025.107616.

Huang, Z.Y., Robinson, G., 1996. Regulation of honey bee division of labor by colony age demography. *Behavioral Ecology and Sociobiology.* 39, 147–158. https://doi.org/10.1007/s002650050276.

IAEA, 2001. Present and Future environmental impact of the Chernobyl accident. IAEA-TECDOC-1240, Vienna, pp. 51–52.

Israel, Y. A., Bogdevich, I. M. (Eds.), (2009). Atlas sovremennyh i prognoznyh aspektov posledstvij avarij na Chernobyl'skoj AJeS na postradavshih territorijah Rossii i Belarusi (ASPA Rossija–Belarus') [Atlas of modern and prognostic aspects of the consequences of the Chernobyl NPP accident on the affected territories of Russia and Belarus (ASPA Russia-Belarus)], Minsk. (In Russian).

Inose, S., Kaseda, T., Hagiwara, K., Honda, T., Koike, Y., Saito, T., 2023. Radioactive analysis of honey samples collected in Japan. Proceedings of the 24th workshop on environmental radioactivity, Tsukuba, pp. 55–58 (In Japanese).

Johnson, B.R., 2010. Division of labor in honeybees: form, function, and proximate mechanisms. *Behavioral Ecology and Sociobiology.* 64, 305–316. https://doi.org/10.1007/s00265-009-0874-7.

Kaste, J.M., Volante, P., Elmore, A.J., 2021. Bomb ^{137}Cs in modern honey reveals a regional soil control on pollutant cycling by plants. *Nature Communications.* 12, 1937. https://doi.org/10.1038/s41467-021-22081-8.

Kendall, L.K., Mola, J.M., Portman, Z.M., Cariveau, D.P., Smith, H.G., Bartomeus, I., 2022. The potential and realized foraging movements of bees are differentially determined by body size and sociality. *Ecology.* 103(11), e3809. https://doi.org/10.1002/ecy.3809.

Lovrenčić Mikelić, I., Ernečić, G., Barišić, D., 2024. Natural and Anthropogenic Radionuclides in Soil around coal-fired Plomin Thermal Power Plant (Istria, Croatia): What Is the Plant Influence and What Controls it? *Fuel.* 371, 131971. https://doi.org/10.1016/j.fuel.2024.131971.

Meteostat, 2025. Weather and climate database [dataset]. https://meteostat.net/ (accessed 2025 May 17).

Meacci, S., Corsi, L., Santecchia, E., Ruschioni, S., 2025. Harnessing Electrostatic Forces: A Review of Bees as Bioindicators for Particulate Matter Detection. *Insects*. 16(4), 373. https://doi.org/10.3390/insects16040373.

PalDat, 2024. Palynological Database: Society for the Promotion of Palynological Research in Austria [dataset]. https://www.paldat.org/ (accessed 2025 May 17).

Palmer, J., Samuelson, A.E., Gill, R.J., Leadbeater E., Jansen, V.A., 2024. Foraging distance distributions reveal how honeybee waggle dance recruitment varies with landscape. *Communications Biology.* **7**, 1306. https://doi.org/10.1038/s42003-024-06987-9.

Prado, A., Requier, F., Crauser, D., Le Conte, Y., Bretagnolle, V., Alaux, C., 2020. Honeybee lifespan: the critical role of pre-foraging stage. *Royal Society Open Science.* 11;7(11), 200998. https://doi.org/10.1098/rsos.200998.

Radchenko, V.G., Pesenko, Y.A., 1994. Biology of bees (Hymenoptera, Apoidea). Saint Petersburg. (In Russian). https://doi.org/10.13140/2.1.3938.6242.

Russian Federation, 1991. On Social Protection of Citizens Exposed to Radiation Due to the Catastrophe at the Chernobyl Nuclear Power Plant: Law of the Russian Federation No. 1244-1 dated 15 May 1991. Moscow. (In Russian).

Russian Federation, 2023. Order of the Government of the Russian Federation No. 745-r dated 28 March 2023. Moscow (In Russian).

Sorokin, P.G., 2025. Calculation of the area per landscape type for determining the weighted average activity concentration of ^{137}Cs in plants [dataset]. Mendeley Data, v4 (2025), https://doi.org/10.17632/nb2w7w9zc2.4.

Svečnjak, L., Chesson, L.A., Gallina, A., Maia, M., Martinello, M., Mutinelli, F., Waters, T.A. et al., 2019. Standard methods for Apis mellifera beeswax research. *Journal of Apicultural Research.* 58(2), 1–108. https://doi.org/10.1080/00218839.2019.1571556.

Vorobyev, G.T., Guchanov D.E., Markina Z.N., Novikov A.A., Kalatskiy V.S., Karpechenko S.V., 1994. Radioaktivnoe zagrjaznenie pochv Brjanskoj oblasti [Radioactive contamination of soils in the Bryansk region]: Monograph. Bryansk, pp. 8–14, 116. (In Russian).

Vearrier, D., Curtis, J. A., Greenberg, M. I., 2009. Technologically enhanced naturally occurring radioactive materials. *Clinical Toxicology.* 47(5). https://doi.org/10.1080/15563650902997849.

Wang, K., Li, W., Li, S., Tian, Z., Koefoed, P., Zheng, X.Y., 2021. Geochemistry and cosmochemistry of potassium stable isotopes. *Geochemistry.* 81(3), 125786. https://doi.org/10.1016/j.chemer.2021.125786.